GLOBAL BIOGEOCHEMICAL CYCLES, VOL. 20, GB1S93, doi:10.1029/2005GB002558, 2006

Particulate iron dynamics during FeCycle in subantarctic waters southeast of New Zealand

R. D. Frew,[1] D. A. Hutchins,[2] S. Nodder,[3] S. Sanudo-Wilhelmy,[4] A. Tovar-Sanchez,[5] K. Leblanc,[2] C. E. Hare,[2] and P. W. Boyd[6]

Received 31 May 2005; revised 5 October 2005; accepted 7 December 2005; published 8 March 2006.

[1] The FeCycle experiment provided an SF_6 labeled mesoscale patch of high-nitrate low-chlorophyll (HNLC) water in austral summer 2003. These labeled waters enabled a comparison of the inventory of particulate iron (PFe) in the 45-m-deep surface mixed layer with the concurrent downward export flux of PFe at depths of 80 and 120 m. The partitioning of PFe between four size fractions (0.2–2, 2–5, 5–20, and >20 μm) was assessed, and PFe was mainly found in the >20-μm size fraction throughout FeCycle. Estimates of the relative contribution of the biogenic and lithogenic components to PFe were based on an Al:Fe molar ratio (0.18) derived following analysis of dust/soil from the nearest source of aerosol Fe: the semi-arid regions of Australia. The lithogenic component dominated each of the four PFe size fractions, with medians ranging from 68 to 97% of PFe during the 10-day experiment. The Fe:C ratios for mixed-layer particles were ~40 μmol/mol. PFe export was ~300 nmol m^{-2} d^{-1} at 80 m depth representing a daily loss of ~1% from the mixed-layer PFe inventory. There were pronounced increases in the Fe:C particulate ratios with depth, with a five-fold increase from the surface mixed layer to 80 m depth, consistent with scavenging of the remineralized Fe by sinking particles and concurrent solubilization and loss of particulate organic carbon. Significantly, the lithogenic fraction of the sinking PFe intercepted at both 80 m and 120 m was >40%; that is, there was an approximately twofold decrease in the proportion of lithogenic iron exported relative to that in the mixed-layer lithogenic iron inventory. This indicates that the transformation of lithogenic to biogenic PFe takes place in the mixed layer, prior to particles settling to depth. Moreover, the magnitude of lithogenic Fe supply from dust deposition into the waters southeast of New Zealand is comparable to that of the export of PFe from the mixed layer, suggesting that a large proportion of the deposited dust eventually exits the surface mixed layer as biogenic PFe in this HNLC region.

Citation: Frew, R. D., D. A. Hutchins, S. Nodder, S. Sanudo-Wilhelmy, A. Tovar-Sanchez, K. Leblanc, C. E. Hare, and P. W. Boyd (2006), Particulate iron dynamics during FeCycle in subantarctic waters southeast of New Zealand, *Global Biogeochem. Cycles*, *20*, GB1S93, doi:10.1029/2005GB002558.

1. Introduction

[2] Iron has been demonstrated to be the nutrient limiting primary productivity in high-nitrate low-chlorophyll (HNLC) regions of the open ocean [*Martin et al.*, 1994; *Coale et al.*, 1996; *de Baar and Boyd*, 1999; *Boyd et al.*, 2000, 2004a], and plays a role in controlling the rate of nitrogen fixation in low-latitude oligotrophic oceans [*Mills et al.*, 2004]. There is also tantalizing evidence from Antarctic ice core records implying that glacial era increases in Southern Ocean macronutrient utilization and in the export of particulate organic carbon (POC) to the deep ocean may be attributed to increases in aeolian iron flux [*Kumar et al.*, 1995; *Watson et al.*, 2000]. Recently, several studies using mesoscale iron enrichment of HNLC waters have investigated the impact of iron supply on the downward POC flux from the surface ocean [*Boyd et al.*, 2004a; *Buesseler et al.*, 2004]. The influence of iron enrichment on

[1]Department of Chemistry, University of Otago, Dunedin, New Zealand.
[2]Graduate College of Marine Studies, University of Delaware, Lewes, Delaware, USA.
[3]National Institute of Water and Atmospheric Research, Wellington, New Zealand.
[4]Marine Sciences Research Center, Stony Brook University, Stony Brook, New York, USA.
[5]Instituto Mediterraneo de Estudios Avanzados (IMEDEA), Mallorca, Spain.
[6]National Institute of Water and Atmospheric Research, Centre for Chemical and Physical Oceanography, Department of Chemistry, University of Otago, Dunedin, New Zealand.

0886-6236/06/2005GB002558

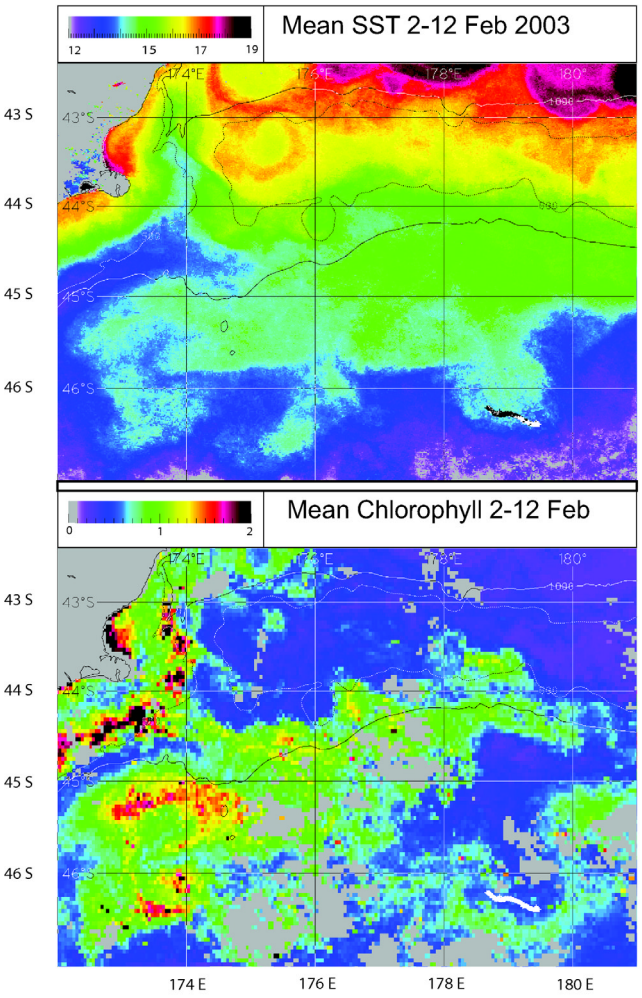

Figure 1a. The trajectories of both surface-tethered free-drifting sediment trap arrays deployed in FeCycle overlaid (white pixels denoted by arrows) onto satellite composite (2–12 February 2003) images of (top) sea surface temperature and (bottom) SeaWiFS chlorophyll ($\mu g\ L^{-1}$).

downward POC export is a key issue in answering whether increased iron supply will elevate carbon sequestration to the deep ocean [e.g., *Martin*, 1990]. Recent modeling studies on large-scale iron fertilization indicate that the fate of iron added to the ocean (i.e., recycled or exported) will also strongly influence how iron supply impacts the sequestration of carbon to depth [*Gnanadesikan et al.*, 2003].

[3] The majority of research into the biogeochemical cycle of iron has focused on dissolved iron (DFe) [*Martin et al.*, 1989; *Johnson et al.*, 1997; *de Baar and de Jong*, 2001; *Wu and Boyle*, 2002] even though the surface mixed-layer pool of total dissolvable iron is dominated by the particulate fraction [*de Baar and de Jong*, 2001]. Studies into the biogeochemical cycles of particles for other elements, such as nitrogen [*Tréguer et al.*, 2003] and silicon [*Ragueneau et al.*, 2000] demonstrate that information is required on particle dynamics to develop an understanding of the links between pools and fluxes, mixed-layer residence time, remineralization and export efficiencies. Little of this information is presently available for PFe. The PFe pool in the surface ocean is comprised of biogenic, lithogenic and detrital iron [*Price and Morel*, 1998]. The main focus on the lithogenic component has been on atmospheric deposition rates of aerosol iron [*Jickells and Spokes*, 2001], and solubilization of the Fe contained within the mineral phase [*Spokes and Jickells*, 1996]. Several studies have attempted to construct biogenic iron budgets for surface waters in HNLC regions [*Price and Morel*, 1998; *Tortell et al.*, 1999; *Bowie et al.*, 2001] and in the Sargasso Sea [*Tortell et al.*, 1999]. However, these budgets have relied heavily on data from algal cultures, and virtually nothing is known, for example, about what constitutes detrital iron or what size this pool is. Recent advances in examining the biogeochemistry of PFe in the ocean include the use of an oxalate wash to remove extracellularly bound iron [*Tovar-Sanchez et al.*, 2003], and the application of synchrotron-based X-ray Fluorescence [*Twining et al.*, 2004] to determine the iron content of individual particles. However, little is known at present about the size distribution of the various components of PFe.

[4] There have been even fewer direct estimates of the downward particle flux of iron from the surface ocean, relative to the number of studies of suspended PFe concentrations. Particle flux estimates have been made using either sediment traps or modeling approaches. Sediment trap measurements of PFe flux in the upper ocean have been mainly restricted to coastal or shelf environments (e.g., Antarctic Peninsula [*Martin*, 1990] or the Gotland Basin [*Pohl et al.*, 2004]). Estimates of PFe export in offshore waters have relied on deep-moored sediment traps (e.g., North Atlantic [*Kuss and Kremling*, 1999]; western Mediterranean Sea [*Quétel et al.*, 1993]). Early studies estimated downward PFe flux using proxies for Fe [e.g., *Collier and Edmond*, 1984]. The majority of recent estimates of PFe export have come from simple models in conjunction with large data sets of DFe [*Johnson et al.*, 1997], or using two compartment box models [*Sherrell and Boyle*, 1992; *Sarthou and Jeandel*, 2001]. The dearth of measurements on key aspects of PFe dynamics, such as links between pools and fluxes, mixed-layer residence time, and remineralization and export efficiencies, has so far delayed progress in developing more detailed iron biogeochemical models [*Fung et al.*, 2000].

[5] Here we present data on the PFe inventory in the surface mixed layer, and the downward export flux of PFe below the mixed layer obtained concurrently from an SF_6 labeled mesoscale patch experiment that show the importance of biological utilization of lithogenic Fe in HNLC subantarctic waters.

2. Methods and Materials

2.1. Study Location

[6] The FeCycle study took place over 10 days (2 to 11 February 2003) at a site east of New Zealand in HNLC waters (46.24°S 178.72°E, Figure 1a). Around 50 km^2 of the upper ocean was labeled with SF_6 (but no iron was added) and the patch areal extent and evolution was monitored daily by underway mapping. For further details of the site selection and patch evolution see *Boyd et al.*

Table 1a. Fe Blank Data for Filters From Trap Deployment[a]

Sample Type	Diameter, mm	Material	Blank/Filter, nmol	Blank/cm^2, pmol
Oxalate-washed mixed-layer PFe trap samples	47	PC	1.0 ± 0.2	58
Mixed-layer PFe	142	PC	0.9 ± 0.2	6
Mixed-layer PFe	142	nylon	1.9 ± 0.3	12

[a]PC denotes polycarbonate. Filter values are average ±1 S.E.

[2005]. Water was sampled daily (at local dawn) from 10 m depth, and also on several days over the diel cycle from the mixed layer at the patch center (defined by the highest daily SF_6 concentrations) using clean techniques (P. L. Croot et al., The importance of physical mixing processes for understanding iron biogeochemical cycling: FeCycle, submitted to *Marine Chemistry*, 2005) (hereinafter referred to as Croot et al., submitted manuscript, 2005).

2.2. Mixed-Layer Particulate Iron Samples

[7] Samples were obtained on 7 February 2003 (at 0830, 1200, 1900 and 2230 hours local time), 8 February (0530 hours), 9 February (0530 hours), and 11 February 2003 (0600, 1000, 1400, 1800 and 2200 hours) using an epoxy-coated towed fish (with an attached plastic-coated RBR© temperature and pressure logger) deployed at 10 m depth in the surface mixed layer and 5 m perpendicular (using a boom) from the vessel. Seawater was pumped directly into the clean container laboratory by an all-Teflon pump (Almatec SL20) through polyethylene tubing. Teflon fittings (Swagelok) were used for all joints. All components of the sampling system that would contact the sample were thoroughly cleaned with dilute quartz-distilled HCl (qHCl). DFe samples collected using the same supply system showed negligible contamination (Croot et al., submitted manuscript, 2005).

[8] Up to 10 L/min of clean seawater was pumped directly into the laminar flow bench of the clean lab container. Samples for PFe were collected on 142-mm-diameter filters in series (20-, 5-, 2- and 0.2-μm pore sizes). The sum of these fractions provided an estimate of total PFe concentration. All filters were polycarbonate (PC) except for the 20-μm pore size which was nylon. Filters were cleaned by soaking in 10% qHCl prior to use. Field blanks, obtained by treating filters exactly as sample filters except for the filtering of a sample, are presented in Tables 1a and 1b. During sample filtration, flow was adjusted to <1 L/min and filtrate collected in 20-L carboys to measure total volume collected (between 50 and 110 L). Filtration continued until the flow stopped, indicating one filter was blocked. Filters were stored frozen in polypropylene vials. They were freeze-dried and their trace element composition quantified after acid-digestion (HNO_3/HF) on a Thermo-Finnigan Element II ICP-MS at the Marine Sciences Research Center, Stony Brook University.

[9] For FeCycle, total biogenic PFe is defined as the difference between the total PFe and lithogenic PFe. The lithogenic component of the PFe was calculated by assuming all the particulate Al (PAl) derives from lithogenic material and multiplying this term by a molar abundance ratio (Fe/Al) of 0.18 based on our data for Australian dust samples (Table 2). This crustal abundance ratio is comparable to the global average for upper continental crust (0.19) reported by *Wedepohl* [1995]. The results of these calculations are presented in Table 3.

[10] Samples for other particulates such as POC and particulate organic nitrogen (PON) were sampled as for PFe, and then collected by filtration onto precombusted 13-mm-diameter glass fiber A/E filters. Filters were dried at 60°C on board the vessel and later analyzed in the laboratory using a Carlo-Erba NA1500 elemental analyzer interfaced to a Europa 20-20 Update mass spectrometer using standard techniques [*Minagawa et al.*, 1984]. Samples for particulate biogenic silica (BSi) were filtered onto 0.6-μm porosity 47-mm-diameter Nuclepore© PC membranes, and dried on board for 24 hours at 60°C. BSi was analyzed in the laboratory following procedures of *Nelson et al.* [1989]. For particulate organic phosphorus (POP) determinations, samples were filtered onto combusted 25-mm-diameter GF/F glass fiber filters, rinsed twice with 2 mL of 0.017 M Na_2SO_4, placed in a combusted glass scintillation vial with 2 mL of 0.017 M $MgSO_4$, and evaporated to dryness on board at 60°C. Vials were then returned to the laboratory and baked at 450°C for 2 hours. After cooling, 5 mL of 0.2 M HCl was added to each vial, which were then tightly capped and heated at 80°C for 0.5 hours. Dissolved phosphate from the digested POP samples was then measured colorimetrically using a spectrophotometer [*Lebo and Sharp*, 1992]. Blank filter values were determined by washing identically combusted GF/F filters mounted on our filter towers with filtered seawater used to process samples. Following analysis, these values were then subtracted from sample values.

2.3. Oxalate-Washed Particulate Iron Samples

[11] Additional samples for mixed-layer PFe concentrations were collected at selected stations using the clean pump system, and were washed using the oxalate technique

Table 1b. Fe Blank Data for Procedural Blanks From Trap Deployment[a]

Sample	Unwashed	Oxalate Washed
F1-80	1.4	1.2
F1-80	2.1	...
F1-120	1.9	1.8
F1-120	...	1.4
F2-80	1.8	1.2
F2-80	...	1.5
F2-120	3.6	1.7
F2-120	...	1.5

[a]Units are nmol/trap cylinder. PC denotes polycarbonate. F1 and F2 refer to two identical trap arrays deployed near the center of the FeCycle patch with fluxes measured at 80 and 120 m water depths.

Table 2. Trace Metal Concentrations of Dry Sieved Dust Samples From the Semi-Arid Regions of Australia[a]

	Sample Identifier	
Metal	Otago 146.1	Thargo 44-53
Pb	1.39×10^4	0.92×10^4
Co	2.1×10^4	0.88×10^4
Cu	2.5×10^4	1.43×10^4
Fe	3.18×10^7	1.78×10^7
Ni	2.53×10^4	1.24×10^4
V	1.04×10^5	0.63×10^5
Zn	4.6×10^4	2.77×10^4
Mn	5.54×10^5	2.53×10^5
Al	8.41×10^7	4.46×10^7

[a]Metal concentrations are in units of ng/g. Dry sieved samples are from 44- to 53-μm fraction. Otago 146.1 denotes a dust sample derived from a laboratory abrasion chamber, and Thargo 44-53 denotes a sieved soil sample from Queensland, Australia.

of *Tovar-Sanchez et al.* [2003]. Pools determined by oxalate wash were the ''intracellular'' pool (PFe following oxalate washing) and the ''extracellular'' pool (total PFe as described in section 2.2 minus the intracellular PFe pool). These values thus represent Fe scavenged onto particle surfaces (extracellular) or incorporated into interior particle matrices (intracellular). Samples were processed using an acid-washed 47-mm-diameter polyethylene ''sandwich-type'' filtration apparatus. PC filter pore sizes used were 20, 5, 2.0 and 0.2 μm, although owing to particle loading issues, many filters ruptured, meaning not all size fractions were obtained in each collection. The volume filtered was assessed by measuring the amount of seawater passing through each filter, and ranged from 2 to 13 liters. Immediately following collection, the oxalate wash was injected into each filter tower using an acid-washed syringe, was left for 5 min before being followed by three rinses with clean, filtered (0.2 μm) seawater. Filter samples were stored frozen in acid-washed plastic bags until digestion and analysis. Samples were digested in aqua-regia-washed Teflon bottles at 60°C for 48 hours using 5 mL concentrated triple-distilled HNO_3. Following digestion, the upper 4 mL was carefully drawn off with a pipettor to avoid removal of the settled particulates and taken to dryness in a laminar flow hood before reconstitution in 0.1M HNO_3 for ICP-MS analyses. All manipulations were carried out within a Class-1000 cleanroom. A subset of PFe samples from the surface-tethered free-drifting traps were also processed using this technique (see section 2.4).

2.4. Downward Particulate Iron Fluxes

[12] The deployment of either deep-moored or free-floating, surface-tethered sediment traps is one of two established methods of measuring downward particle export in the ocean, the other is Uranium-Thorium disequilibria [*Buesseler*, 1991]. The sediment trap approach is not without contentious issues regarding the collection efficiency of sinking particles [*Buesseler*, 1991; *Buesseler et al.*, 2000; *Gust et al.*, 1994; *Gardner*, 2000]. Although the contamination from the metal components, that are often used on sediment traps, is a major issue in trace metal studies, the sediment trap approach rather than the ^{234}Th technique is the only method presently available to directly measure PFe export in the ocean [*Pohl et al.*, 2004].

[13] PFe export from the surface mixed layer was estimated using two arrays of surface-tethered free-drifting sediment traps which were each deployed near the patch centre on February 3 2003. Each array had two traps one at 80-m subsurface and the other at 120 m depth. Trap array 1 and Argos buoy 01957,were deployed at 46.21°S 178.69°E and array 2 (Argos buoy 18634) was deployed at 46.21°S 178.70°E. A 10-m-long bungee line was used on each array to reduce surface wave effects on the traps, and the arrays were designed to minimize wind-driven slippage through the water [*Gardner*, 2000]. Twelve cylindrical traps (7 cm diameter; aspect ratio = 8.29) were placed on the cross frame at each sampling depth. The traps and cross frames are identical in design to those used in the JGOFS Hawaii Ocean Time series program [e.g., *Karl et al.*, 1990]. Four sealed procedural blanks were also attached to the mooring line at each depth on both trap arrays.

[14] The procedural blanks were essential to ensure that the preparation of the trap apparatus, reagents and brine preservatives, which as potential sources of Fe contamination may each contribute to the overall blank, was adequate to provide reliable estimates of PFe export fluxes. Trace metal clean handling techniques were used throughout the preparation of the traps and their deployment, recovery, and subsequent sample handling and filtration. Before deployment, polycarbonate trap cylinders were acid-washed by soaking in 10% qHCl for 2 weeks. Trap cross frames were plastic-welded, cleaned in ethanol and sealed in plastic bags. Nonmetallic line (Spectra) and plastic-coated stainless steel hardware were used for all fittings to minimize contamination. Trap cylinders were filled with 0.2-μm filtered seawater (collected with the system used for sampling water for subsequent trace metal analysis (Croot et al., submitted manuscript, 2005)) in the clean container laboratory 18 hours prior to the deployment then backfilled 12 hours later with a basal brine of chelexed ANALAR NaCl-borax (5‰ excess salinity) to which 50 mL of triple quartz-distilled chloroform had been added [*Knauer et al.*, 1984]. Trap cylinders were then covered with clean plastic bags, held in place by dissolvable links [*Karl et al.*, 1990]. All backfilling and predeployment preparations were undertaken in a laminar flow tent.

[15] The trap arrays were deployed for 7 days and remained either within the SF_6 labeled patch (Figure 1b) or near its periphery (i.e., within HNLC waters, Figure 1a), both drifting to the southeast of the deployment site. Both arrays were recovered on 10 February: at 1311 hours for array 1 (46.41°S 179.23°E) and 1500 hours for array 2 (46.39°S 179.47°E). Deployment and recoveries were completed under calm sea conditions. Traps were recovered by maneuvering the ship to approach from downwind, and were picked up using the crane at full extension to avoid contamination. The traps were carefully raised to the surface away (i.e., upwind) from the side of the vessel and once in proximity to the ship, each cylinder was capped with clean plastic coverings before removing from the cross-frame.

[16] Trap contents above the 8- to 9-cm-thick basal brine in each cylinder were aspirated off using acid-washed

Table 3. Size-Fractionated Fe and Al Concentrations Within Particulates From the Mixed Layer Within the FeCycle SF_6 Labeled Patch[a]

Sampling Time, days	Filter Pore Size, μm	[PAl], nmol/L	[PFe], nmol/L	Total [PFe], nmol/L	Lithogenic [PFe], nmol/L	Biogenic [PFe], nmol/L	Percent Lithogenic
7.35	0.2	0.51	0.13	0.72	0.09	0.04	71
	2	0.10	0.05		0.02	0.03	40
	5	0.51	0.25		0.09	0.15	38
	20	1.55	0.29		0.29	0.00	98
7.50	0.2	0.67	0.15	0.82	0.13	0.02	84
	2	0.16	0.07		0.03	0.04	40
	5	0.43	0.33		0.08	0.25	24
	20	1.10	0.27		0.20	0.06	77
7.79	0.2	0.34	0.13	0.85	0.06	0.06	50
	2	0.71	0.21		0.13	0.08	64
	5	0.65	0.13		0.12	0.01	95
	20	2.40	0.39		0.45	<0.01	116
7.94	0.2	0.32	0.21	0.94	0.06	0.15	29
	2	0.69	0.20		0.13	0.07	65
	5	0.90	0.22		0.17	0.06	75
	20	1.48	0.31		0.33	0.08	80
8.23	0.2	0.48	0.09	0.67	0.09	0.01	94
	2	0.44	0.08		0.08	0.00	101
	5	0.66	0.16		0.12	0.04	78
	20	1.54	0.33		0.29	0.05	85
8.43	0.2	0.31	0.08	0.58	0.06	0.02	72
	2	0.44	0.09		0.08	0.01	94
	5	0.64	0.10		0.12	<0.01	116
	20	1.45	0.31		0.27	0.04	87
9.23	0.2	0.42	0.11	0.67	0.08	0.04	68
	2	0.43	0.09		0.08	0.01	87
	5	0.54	0.14		0.10	0.04	70
	20	1.77	0.32		0.33	<0.01	102
11.25	0.2	0.48	0.17	0.55	0.09	0.08	54
	2	0.56	0.09		0.10	<0.01	120
	5	0.51	0.08		0.10	<0.01	122
	20	1.14	0.22		0.21	0.00	98
11.42	0.2	0.59	0.15	0.64	0.11	0.04	72
	2	0.53	0.10		0.10	0.00	96
	5	0.61	0.08		0.11	<0.01	-
	20	1.61	0.30		0.30	0.00	99
11.58	0.2	0.76	0.16	0.89	0.14	0.02	87
	2	0.72	0.20		0.13	0.07	65
	5	0.99	0.20		0.18	0.02	92
	20	2.23	0.32		0.31	0.01	97
11.75	0.2	0.24	0.09	0.49	0.05	0.04	52
	2	0.40	0.09		0.07	0.02	83
	5	0.52	0.10		0.10	0.01	91
	20	0.86	0.20		0.16	0.04	78
11.92	0.2	0.51	0.09	0.56	0.10	0.00	102
	2	0.47	0.10		0.09	0.01	91
	5	0.53	0.10		0.10	0.00	99
	20	1.57	0.27		0.29	<0.01	109

[a]Sampling time is in decimal days from the beginning of February 2003. All samples were collected at a depth of 10 m except the sample on day 8.43 which was collected at 25 m depth.

Teflon tubing in the laminar flow, leaving a volume of 300–350 mL. This aspiration process took place within 5–6 hours of recovery. Samples were then prescreened through an acid-washed 200-μm mesh to remove zooplankton "swimmers" prior to filtering [*Karl et al.*, 1990]. Swimmers comprised only a minor component of trap material (<5–10% of biomass). For each trap, the 300–350 mL of trap solution was filtered onto an acid-washed 0.2-μm porosity 47-mm diameter PC filter under a class-100 laminar flow hood using covered acid-washed polyethylene filtration towers. Oxalate-washed samples received a 5-min exposure to the reagent just before the sample filtered dry, followed by three rinses with clean filtered seawater [*Tovar-Sanchez et al.*, 2003]. Seawater-washed samples received the same treatment, but without the oxalate rinse step. Trap samples were prepared as for the suspended PFe samples (see section 2.4) and trace element concentrations were quantified by ICP-MS.

[17] Trace metal procedural blanks were run for both oxalate-washed samples and seawater-washed samples. The trap cylinders used for the blanks consisted of an identical brine/poison solution, deployed and recovered along with the trap cylinders used to intercept particles, but without removing the plastic covering to allow particle collection. Blanks were then subjected to identical filtration and analytical procedures described for the samples. The

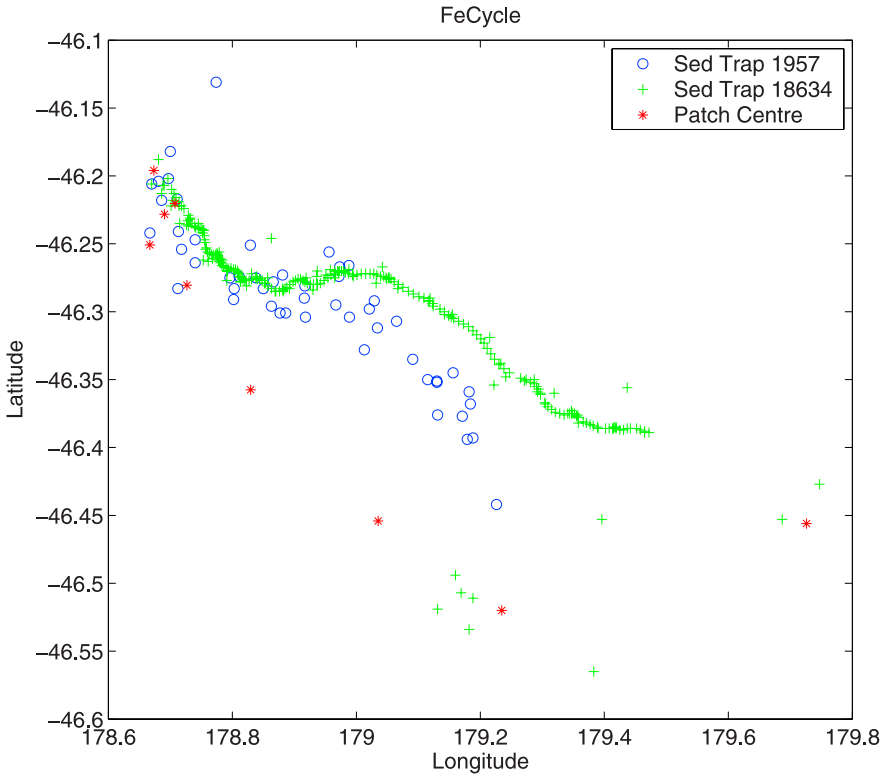

Figure 1b. A plot of the drift trajectories of each trap array in relation to the position of the center of the FeCycle patch determined daily from underway mapping, with the center being at the location of the highest SF_6 concentrations. The SF_6-labeled patch area increased from 50 to 400 km^2 during FeCycle.

average of the two blanks for each treatment was subtracted from the values reported for the appropriate samples.

[18] Problems were encountered performing the oxalate wash on trap samples. The high particulate loading meant filters were run essentially to being completely clogged. The effectiveness of this wash depends on having the rinse access all of the particulate surfaces, and then the reduced Fe must wash away through the filter. It is possible that owing to the very heavy particle load on these filters, the wash either did not remove the "extracellular" Fe efficiently (i.e., not all particle surfaces were evenly exposed to the wash), and/or the removed iron (II) did not rinse through the filters efficiently, and was retained to some extent. Therefore the data on oxalate-washed PFe concentrations presented in Tables 4a and 4b should be regarded as an upper estimate of "intracellular" + lithogenic PFe.

2.5. Downward Particulate C, N, Si, and P Fluxes

[19] POC, PON, POP and BSi fluxes were also obtained from the sediment traps at 80 and 120 m depths. For both sampling depths, in each of the two traps, the volume in one cylinder after aspiration was filtered for POP, and one for BSi. For POC and PON, the contents of two cylinders were filtered, from each depth, for each trap. Analytical blanks consisted of 150 mL of brine and chloroform mixture filtered in the same manner as the particulate samples; these values were subtracted from the reported particulate fluxes. Sample analysis for these particulates is as described for suspended particulate samples in section 2.2.

2.6. Analysis of Soil and Dust Samples

[20] The provenance of lithogenic iron that is episodically deposited into the HNLC waters east of New Zealand is from the arid and semi-arid interior of Australia [*McGowan et al.*, 2000, 2005]. Samples of Australian soil/dust were obtained and analyzed for their elemental abundance (Table 2). Both samples originate from Thargomindah, a region were dust storms are frequently reported [*Mackie et al.*, 2005], about 200 km east of Cannamulla in SW Queensland, Australia. The soil sample was from 0–10 cm depth in soil class Cf3. The dust in the 44- to 53-μm fraction (denoted as Thargo 44–53) was dry sieved from the bulk soil. The second sample (denoted as Otago 146.1) is artificial dust produced in a lab abrasion chamber (D. Mackie, unpublished data, 2005). All trace metal concentrations were quantified using a Thermo-Finnigan Element II ICP-MS after acid digestion (HNO_3/HF) of the sample.

3. Results

3.1. Blanks

[21] The blanks for filters used to sample total mixed-layer PFe were very low (6–12 pmol/cm^2), comparable to those of *Cullen and Sherrell* [1999], who found 14 pmol/cm^2 in acid-cleaned PC filters. The oxalate wash blanks were higher but still <10% of the sample. Procedural blank

Table 4a. Particle Fluxes of Particles Intercepted in Traps Deployed at 80 and 120 m Depth[a]

Particle Fluxes	F1-80 m	F1-120 m	F2-80 m	F2-120 m
POC, mmol m^{-2} d^{-1}	...	2.09 (0.03)	2.51 (0.17)	2.10 (0.01)
PON, mmol m^{-2} d^{-1}	...	0.30 (0.01)	0.41 (0.03)	0.29 (0.01)
POP, μmol m^{-2} d^{-1}	13.1	13.1	15.0	11.6
BSi, μmol m^{-2} d^{-1}	101	90	127	75
TotPFe, nmol m^{-2} d^{-1}	219 (26)	359 (47)	548 (64)	350 (29)
BioPFe, nmol m^{-2} d^{-1}	112 (23)	230 (46)	352 (62)	174 (28)
LithPFe, nmol m^{-2} d^{-1}	107 (3)	129 (14)	196 (3)	176 (2)
$Tot_{oxalate}$PFe, nmol m^{-2} d^{-1}	374 (51)	370 (24)	469 (14)	454 (42)

[a]The mean of two replicates is reported with the standard error in parentheses. F1 and F2 refer to two identical trap arrays, deployed at two different locations. POC, particulate organic carbon; PON, nitrogen; P, phosphorus; BSi, biogenic silica; TotPFe, total iron; Biol, biogenic; Lith, lithogenic; oxalate, oxalate washed. Several cylinders were lost from the 80-m trap on array 1 so no data for POC and PON, and thus for particulate Fe:C or Fe:N ratios, were available.

values for the sediment trap assays averaged ~20% of the measured sample values in each case and were typically around 1.5 nmol. Data on the blanks for both suspended particulate and trap samples are presented in Tables 1a and 1b.

3.2. Suspended PFe Concentrations

[22] Figure 2a presents the time series of mixed layer, size-fractionated PFe. The total PFe (sum of fractions) ranged from 0.49 to 0.94 nmol/L with a median concentration of 0.68 nmol/L. PFe concentrations were generally constant on each of the 2 days when five diel samples were taken. However, on each day there was one outlier which exhibited elevated PFe concentration. From our understanding of particle dynamics it would seem unlikely that such a temporary elevation in concentration would occur within an SF_6-labeled patch. Moreover, no coincident shift in other biological and chemical properties (such as chlorophyll or macronutrients) was observed in the patch during diel sampling [*McKay et al.*, 2005]. Removal of these two outliers from the data analysis has very little effect on the median PFe concentration.

[23] The distribution of suspended PFe between size classes shows a consistent trend, with the possible exception of the first two samples from the 5- to 20-μm size class on February 7. Both these samples had Fe/Al molar ratios more than twice the crustal average indicating they may contain contaminant Fe. They are therefore excluded from the statistical analysis that follows. The three fractions <20 μm had consistently low median concentrations each of ~0.13 nmol/L (standard error (S.E.) = 0.01). The >20-μm fraction had much higher concentrations (median = 0.30 nmol/L, S.E. = 0.02). No obvious diel trends in the size partitioning of PFe are apparent (Figure 2a). These data are presented in Table 3.

3.3. Relative Contributions of the Lithogenic and Biogenic Particulate Iron

[24] The distribution of lithogenic PFe among the size fractions is shown in Figure 2b. The temporal trends in lithogenic PFe mirrors that of the total PFe (Figure 2a) with a consistent size distribution throughout FeCycle. The median lithogenic Fe concentrations, from smallest to largest fraction, were; 0.08, 0.10, 0.12 and 0.29 nmol/L. These data are reasonably consistent with S.E. <0.02 in each case.

[25] The percent lithogenic component of individual size classes (Figure 2c) ranged from 24 to 122% with several extreme values apparent. The proportion of PFe that is lithogenic, when expressed as a percentage, is inherently more variable than data presented as PFe concentration as it encompasses uncertainties in PFe, PAl measurements and the assumption of constant Fe/Al ratio in all lithogenic particles. Taking the median of each size class indicates that lithogenic PFe comprised 68–97% of the total PFe with a trend of increasing lithogenic component with increasing particle size. The smallest particles (0.2–2 μm) were 68 ± 6% lithogenic (mean ± 1 S.E.). The two intermediate sizes (2–5 μm and 5–20 μm) had 86 ± 5% and 93 ± 5% respectively. Particles >20 μm had the greatest proportion of lithogenic Fe at 97 ± 3%. Thus the largest particles made the greatest contribution to the PFe pool and had the highest proportion of lithogenic Fe.

3.4. Intracellular Versus Externally Bound Fe

[26] A comparison of replicate PFe samples that had been oxalate-washed with those that were not washed provides estimates of surface bound Fe by difference and of "intracellular" PFe from the oxalate-washed samples. This approach was used for 17 filters, however as only two complete sets of all four fractions were obtained results are reported for the individual filters compared with their unwashed pair. The concentration of PFe in washed particles ranged from 0.04 to 0.31 nmol/L compared with 0.05 to 0.39 nmol/L for the corresponding

Table 4b. Elemental Ratios of Particles Intercepted in Traps Deployed at 80 and 120 m Depth[a]

Ratios	F1-120 m	F2-80 m	F2-120 m
C:N, mol:mol	7.0	6.1	7.4
C:P, mol:mol	159	168	182
N:P, mol:mol	22.9	27.6	24.6
Si:C, mol:mol	0.04	0.1	0.04
TotPFe:C, μmol:mol	172	218	167
LithPFe:BioPFe, mol:mol	0.56	0.56	1.0
$TotPFe_{oxalate}$:C, μmol:mol	178	187	217

[a]F1 and F2 refer to two identical trap arrays, deployed at two different locations. POC, particulate organic carbon; PON, nitrogen; P, phosphorus; BSi, biogenic silica; TotPFe, total iron; Biol, biogenic; Lith, lithogenic; oxalate, oxalate washed. Several cylinders were lost from the 80-m trap on array 1 so no data for POC and PON, and thus for particulate Fe:C or Fe:N ratios, were available.

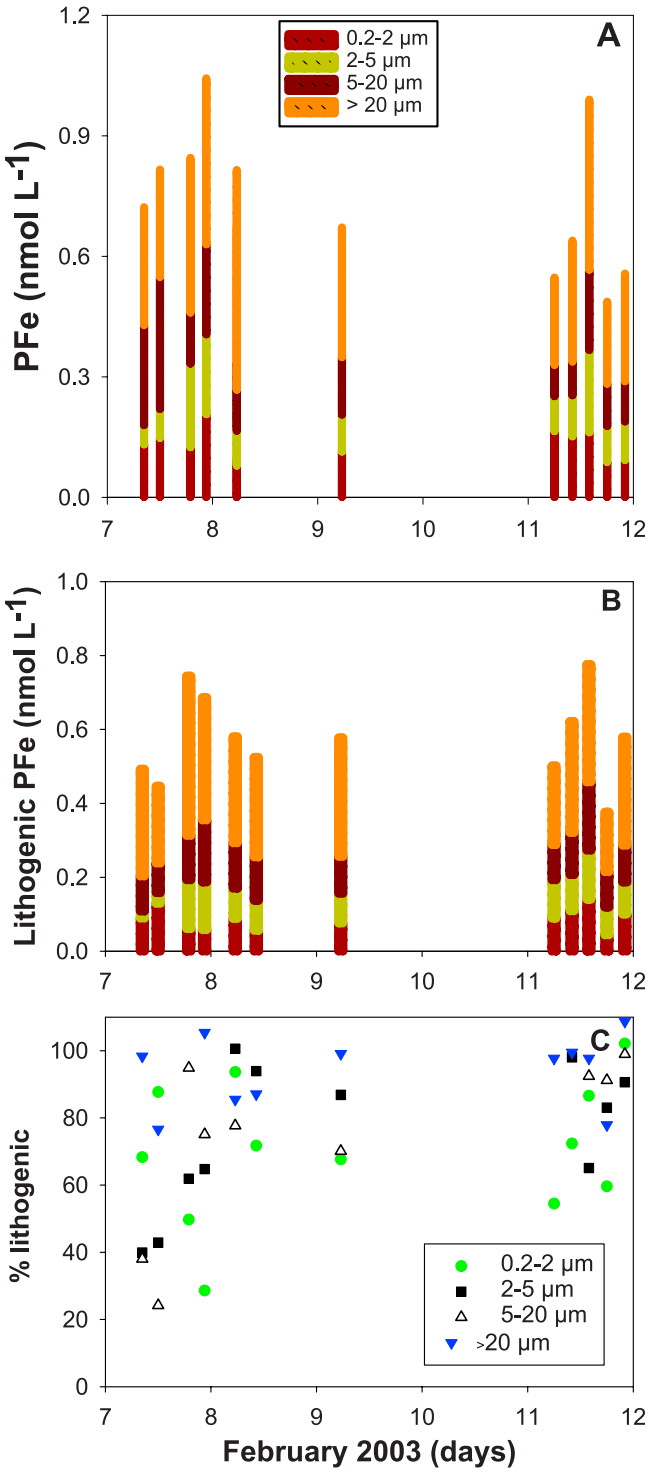

Figure 2. Time series of size-fractionated PFe in the surface mixed layer for (a) total particulate Fe (nmol/L), (b) lithogenic component calculated from particulate Al (Fe/Al = 0.18), and (c) percent contribution of lithogenic to total PFe. Data for these panels are presented in Table 3.

unwashed particles. The average concentration of PFe in the washed fractions was 0.10 ± 0.02 nmol/L. This compares with 0.18 ± 0.03 nmol/L total PFe for unwashed samples. Thus it appears that around 45% of PFe is removed by the oxalate wash and could be classified as "extracellular."

3.5. Sediment Trap Drift Trajectories

[27] The areal extent of the FeCycle patch increased from 49 km^2 to over 400 km^2 during the 10-day experiment [*Boyd et al.*, 2005]. The traps remained near the patch centre for the first 3.5 days of the deployment, but on days 4 and 5 were located on the NE periphery of the patch (Figures 1a and 1b). The traps drifted outside of the patch on day 6 and were around 10 km from the patch periphery on day 7, prior to being recovered. A comparison between the trap trajectories and the chlorophyll field around the FeCycle site (Figure 1a) indicates that although the traps were outside of the patch for 2 days of the 7-day deployment they did not cross any pronounced lateral gradients of elevated chlorophyll concentration that may have resulted in increased downward particulate flux.

3.6. Downward PFe Fluxes

[28] The flux of particles intercepted by each sediment trap are presented in Table 4a. At 80 m depth, total PFe export was 219 ± 13 nmol m^{-2} d^{-1} for array 1 and 550 ± 65 nmol m^{-2} d^{-1} for array 2. In contrast, there was good agreement between the 120 m arrays for the PFe fluxes which were both around 350 ± 40 nmol m^{-2} d^{-1}. Thus the trends in PFe export with depth differ between arrays, with an increase in downward flux for array 1, and a 35% attenuation in the PFe flux signal between 80 m and 120 m depth for array 2. Fluxes of POC, PON, POP and BSi showed differing degrees of vertical attenuation between 80 and 120 m depths that reflect different remineralization length scales for each element. The most rapid attenuance of the downward particle flux (i.e., the shortest remineralization length scale) was recorded for both PON and BSi (both 27%), followed by POC (16%) and POP (12%). The degree of vertical attenuation in the export signal of these elements was more marked for array 2 than array 1, with the 80-m POP flux being 30% less than that at 120 m in array 2 (compare identical POP fluxes at both depths in array 1). This, along with a relatively low PFe flux at 80 m in array 1 compared with array 2, may be indicative of undertrapping of particles by the 80 m trap in array 1. Also note the much higher PFe flux obtained from the oxalate-washed samples from array 1 at 80 m; the oxalate-washed flux should be lower than the total PFe flux, further indicating an underestimation of PFe flux by the 80 m trap on array 1.

[29] The lithogenic portion of the PFe export flux was calculated from the PAl using an Fe:Al molar ratio of 0.18 (see section 3.3). The lithogenic portion was 49% for array 1 and 36% for array 2 of the total exported PFe at 80 m, while at 120 m there was 36% lithogenic PFe for array 1 and 50% for array 2. Thus there is no evidence here for change in% lithogenic composition of PFe between 80 and 120 m. However, the 43% lithogenic character of exported

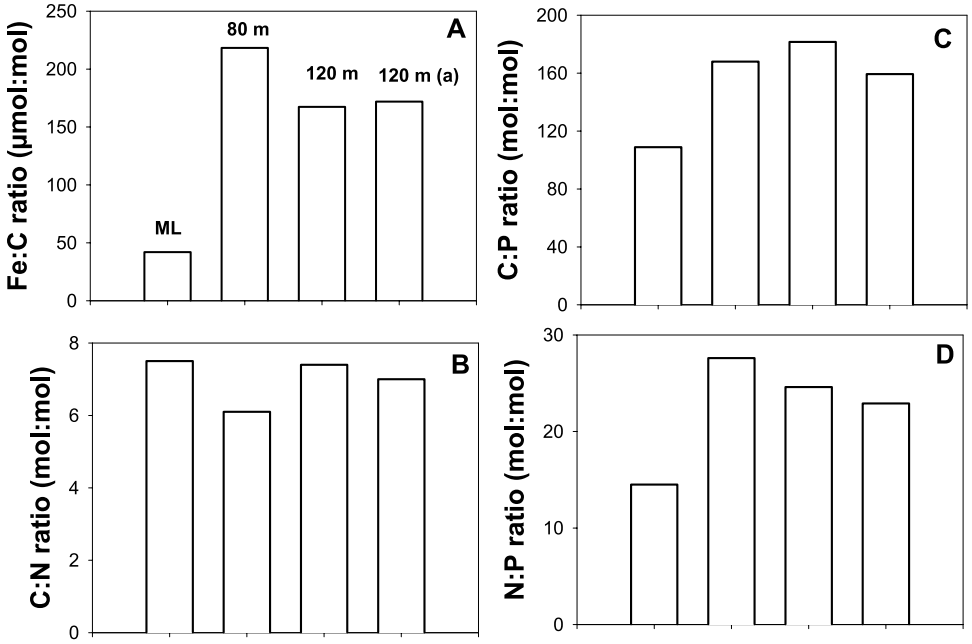

Figure 3. Elemental molar ratios of surface mixed layer and sinking particulate material intercepted in traps at 80 and 120 m depth. (a) Fe:C. (b) C:N. (c) C:P. (d) N:P. ML denotes surface mixed layer, 80 m and 120 m denote the trap depths on array 2, and 120 m(a) denotes the trap depth on array 1. No data were available for POC or PON fluxes for the 80 m trap on array 1.

PFe contrasts strongly with the near 90% lithogenic contribution found in the suspended particles (section 3.3).

[30] Figure 3 compares the elemental ratios of the suspended particles from the surface mixed layer with those of the sinking particles intercepted at the two trap depths. The most striking variation is seen in the Fe:C ratios which increase fivefold from 42 μmol/mol in the surface mixed layer to a maximum of 218 at 80 m then decrease to 169 at 120 m. The C:P and N:P ratios (mol/mol) also increased from the surface layer (108, 14) to 80 m (168, 28) with little change from 80 m to 120 m (170, 24). The C:N ratio decreased from 7.5 mol/mol in the surface layer to 6.1 at 80 m and increased again to 7.2 at 120 m.

4. Discussion

4.1. Characteristics of the Suspended Particulate Iron Pool

4.1.1. Total POC and PFe Concentrations

[31] Macronutrient and chlorophyll concentrations for the FeCycle patch show that the region was HNLC for the entire experiment [*Boyd et al.*, 2005]. Concentrations of POC and other suspended particulates were comparable to those reported previously for these subantarctic waters SE of New Zealand [*Bradford-Grieve et al.*, 1999; *Nodder and Northcote*, 2001].

[32] FeCycle provided the first estimates of total PFe for subantarctic waters SE of New Zealand. The range of total PFe concentrations measured (0.49–0.94; median = 0.68 nmol/L) is generally slightly higher than the total Fe concentration of 0.5 nmol/L reported for the mixed layer during FeCycle by Croot et al. (submitted manuscript, 2005). Croot et al.'s results were obtained from measurements of the acid-labile (pH < 2) component of unfiltered water samples and would probably not have included the entire refractory PFe component. There are few other estimates of total suspended PFe for HNLC waters. Reported concentrations range from 0.15 to 0.9 nmol/L, these are summarized in Table 5.

4.1.2. Size Partitioning of PFe

[33] Although total PFe concentrations have been reported in several studies (Table 5), there is a paucity of data on the partitioning of PFe within size fractions. At present, most of the focus on size fractionation of iron has been at the kDa scale (i.e., <0.2 μm) found in the "dissolved" class [e.g., *Nishioka et al.*, 2001]. This focus is surprising as it has long been recognized that a predictive understanding of trace metal behavior requires a detailed quantitative description of dissolved/particulate interactions, and of the export of particles through the water column [*Sherrell and Boyle*, 1992]. The only other detailed study of size-fractionated PFe, we are aware of is that of *Weinstein and Moran* [2004]. They size-fractionated mixed-layer samples (20 m depth) from the Labrador Sea into three classes and reported PFe concentrations of ∼0.2 nmol/L (0.4–10 μm); ∼1 nmol/L (10–53 μm) and ∼0.5 nmol/L (>53 μm).

[34] Throughout FeCycle, the lowest concentration of PFe was consistently in the three smallest size classes, with the PFe in >20 μm size class always containing the highest PFe concentration, close to half the total PFe. Owing to the different size fractions used by *Weinstein and Moran* [2004] in the Labrador Sea and during FeCycle it is not possible to compare these trends further.

Table 5. Summary of Reported Concentrations of PFe From HNLC Mixed-Layer (0–50 m) Waters[a]

Region	Sample Type	[Fe], nmol/L	Source
Southeast Pacific	acid-labile	0.5	Croot et al. (submitted manuscript, 2005)
Northeast subarctic Pacific	total suspended	0.6	*Price and Morel* [1998]
Ross Sea	particulate	0.2–0.5	*Martin et al.* [1990]
Bellinghausen Sea	total dissolvable	<0.1–0.5	*de Baar et al.* [1999]
HNLC equatorial Pacific	particulate	0.2–0.5	*Gordon et al.* [1998]
Pacific Sector Southern Ocean	particulate	0.9	*Tovar-Sanchez et al.* [2003]
Pacific Sector subantarctic front	particulate	0.7	*Tovar-Sanchez et al.* [2003]

[a]Sample type denotes the definition given in the reference for the component analyzed.

4.1.3. Lithogenic and Biogenic PFe

[35] The lithogenic Fe component dominated the PFe pool in the surface mixed layer during FeCycle, comprising 68–97% of PFe, whereas *Sherrell and Boyle* [1992] reported that the aluminosilicate contribution to total PFe at depths >1000 m in the Sargasso Sea to be <15%. The main source of these lithogenic Fe particles is probably the arid and semi-arid regions of Australia via dust transport [*McGowan et al.*, 2005]. However, the high lithogenic proportion is perhaps surprising given that the source region is >1500 km west of the FeCycle site. Furthermore, there is a marked attenuation in the dust load (i.e., a halving) that is atmospherically transported, termed the 1/2 decrease distance [*Prospero et al.*, 1989], in this region that may be as low as 500 km owing to the higher humidity that characterizes the air masses above the Southern Ocean relative to lower latitudes [*Boyd et al.*, 2004b]. Our estimate of total biogenic PFe (based on an observed Fe:Al crustal abundance molar ratio of 0.18) was 0.14 nmol/L. This is consistent with *Strzepek et al.* [2005] who independently estimated, using Fe:C ratios and biomass data on microheterotrophs and phytoplankton, that the biogenic PFe pool in the mixed layer during FeCycle was 0.12 nmol/L. This biogenic Fe concentration is relatively high for HNLC waters [*Strzepek et al.*, 2005].

4.1.4. Size Partitioning of Lithogenic and Biogenic PFe

[36] The majority of PFe in each of the size fractions during FeCycle was lithogenic. The 0.2- to 2-μm fraction having the least (68%) and the proportion increasing to 95% in the >20-μm particles. Biogenic PFe was mainly in the 0.2- to 2-μm size fraction [*Strzepek et al.*, 2005]. Data on the size partitioning of lithogenic PFe in the surface ocean potentially provide insights into transformations of this lithogenic component within the surface mixed layer. However, they must be carefully compared with the size spectra of atmospheric dust particles.

[37] There is a wide range of particle sizes which have been reported to dominate dust samples with both large (i.e., >100 μm diameter transported across the NW Pacific [*Betzer et al.*, 1988]) and small (i.e., 4–5 μm diameter for Saharan dust at source [*Jickells and Spokes*, 2001]) being recorded. Air mass back trajectories from the FeCycle site (Figure 4) are indicative of the potential supply of dust from the semi-arid and arid regions of Australia over the south of New Zealand in early February 2003. *Hesse and McTainsh* [1999] report size spectra for dust from central Australia that show the majority of the suspended or dispersed dust at source occurs in the 2- to 10-μm size range. Presumably, over the >1500 km traveled by dust to be deposited at the FeCycle site we would see a marked decrease in the mean size [*Jickells and Spokes*, 2001]. On the basis of a "half-decrease distance" of 500 km for this region by the time the (hypothetical) air mass reached the FeCycle site from Australia (Figure 4) ~90% of its dust load would have been lost through deposition. That the largest pool of lithogenic PFe in FeCycle was in the >20 μm size (Table 4a) which contained approximately half of the total PFe is therefore surprising. Thus the partitioning of lithogenic iron during FeCycle across each of the four size fractions indicates transformations of lithogenic dust within the mixed layer by a range of processes (Figure 5). More information is required on the size spectra of dust particles entering HNLC waters to determine what changes

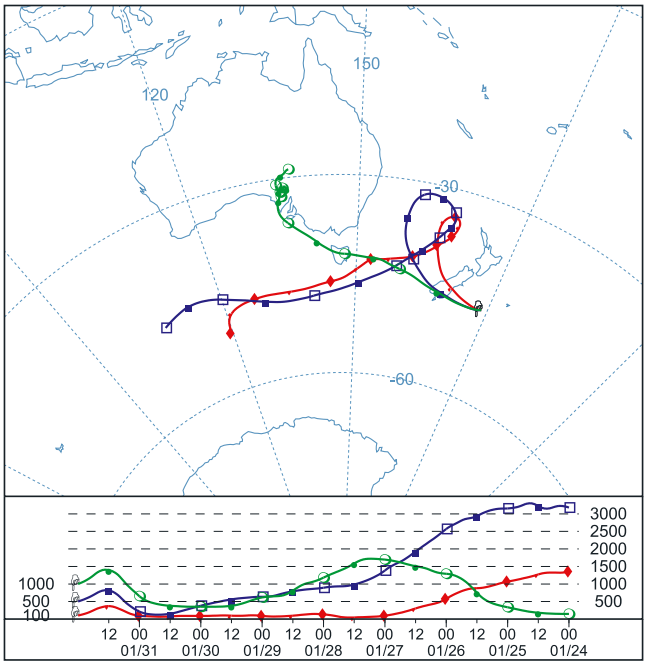

Figure 4. Indirect evidence of the potential for the propagation of dust from the semi-arid and arid regions of Australia over the FeCycle site SE of New Zealand in early February 2003 based on air mass back trajectory analysis (see *Boyd et al.* [2004b] for details). During this period, there was evidence of enhanced aerosol activity in the Tasman Sea (see satellite remote sensing images from Total Ozone Mapping Spectrometer (TOMS) shone by *Boyd et al.* [2005]).

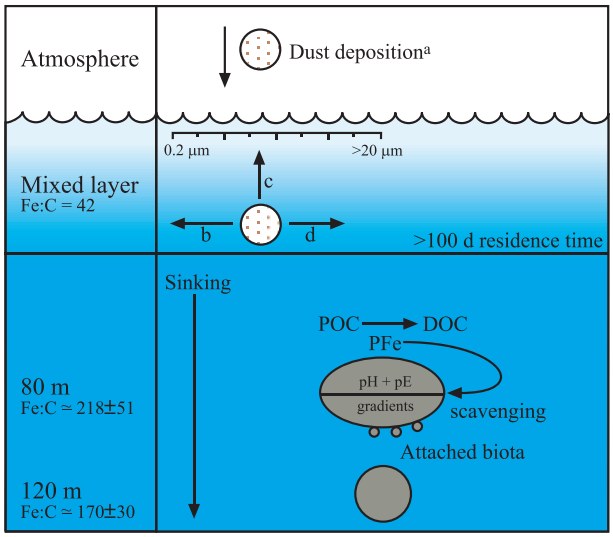

Figure 5. Schematic of potential mechanisms involved in the transformations of lithogenic to biogenic PFe within the surface mixed layer, and the subsequent alteration of the Fe:C ratio in sinking particles upon exiting the surface mixed layer. (a) Dust deposition of small particles (in some cases of 5 μm or less (see *Jickells and Spokes* [2001] but also see *Betzer et al.* [1988])) into the surface ocean. Examples of potential transformation mechanisms to alter the size structure of this lithogenic Fe are denoted by (b) dissolution of iron hydroxides by heterotrophic bacteria leading to reduction in the particle size of PFe, (c) phagotrophy by micrograzers resulting in no change in the PFe size spectrum, and (d) incorporation into larger heterogeneous biological particles leading to increased particle sizes of PFe. Below the mixed layer, the observed increases in particulate Fe:C ratios to 80 m depth are probably due to the rapid microbial solubilization of sinking particles resulting in the conversion of POC to DOC, whereas for PFe the remineralized iron is probably rapidly rescavenged by settling particles.

in size partitioning of Fe may occur owing to such particle transformation processes.

4.1.5. Particulate Fe:C Ratios

[38] The mixed-layer PFe:POC ratio of 42 μmol:mol (mean) is higher than the algal Fe:C ratios of 6–14 μmol:mol reported by *Twining et al.* [2004] for HNLC polar waters south of New Zealand. The PFe:POC ratio for FeCycle is at the upper bound of the Fe:C ratios reported by *Tovar-Sanchez et al.* [2003] for HNLC subantarctic waters south of Australia. However, as 68–95% of the mixed-layer PFe was lithogenic during FeCycle, the biogenic PFe:POC ratio would be lower, around 4 to 12, which is comparable to those reported for algal Fe:C ratios by *Twining et al.* [2004].

4.1.6. "Intracellular" Versus "Extracellularly" Bound Fe

[39] *Hudson and Morel* [1989] developed a titanium wash to remove "extracellular" Fe from phytoplankton lab cultures thus distinguishing "intracellular" from "extracellularly bound" Fe. *Tovar-Sanchez et al.* [2003] subsequently produced an Fe-clean oxalate wash and applied it to natural samples that include phytoplankton, but also detrital and other planktonic material. The oxalate wash provides a means of estimating the amount of Fe in the scavenged pool (i.e., loosely adhering to the exterior of the cells) and thus the intracellular PFe pool (by difference). However, caution must be taken in the definition of "intracellular" and "extracellular" Fe when applied to natural samples. Algal culture samples are dominated by biogenic Fe with little, if any, lithogenic Fe. This is not the case for FeCycle samples which contain predominantly lithogenic PFe likely comprising several components from loosely adsorbed Fe-oxyhydroxides to refractory mineral phases.

[40] Although we could only compare results for individual size fractions (owing to filter rupturing issues; see section 2) for the FeCycle samples, this comparison indicated that 56% of the PFe was in the "intracellular" or refractory mineral pools; that is, ~44% of PFe was removed by washing. Only one other published study, in subantarctic HNLC waters south of Australia [*Tovar-Sanchez et al.*, 2003], has presented results using this approach. Their results indicate that surface-adsorbed Fe accounted for 86% (47°S 145°E) and 50% (51°S 144°E) of the total PFe at each location. Our results imply that a significant portion of the Fe defined as lithogenic (a mean of 82% of PFe was lithogenic compared to 44% of PFe removed by the oxalate wash) must be removed by the surface wash and/or was "intracellular." Therefore approximately 50% of the lithogenic material was removed from particle surfaces. At present, it is not known whether the oxalate wash discriminates between biogenic PFe bound to the particle's exterior or lithogenic PFe not combined with organic particles, i.e., mineral grains. Reports of "hot spots" of lithogenic iron on heterogeneous (i.e., lithogenic and biogenic) particles [*Lam et al.*, 2004; *Twining et al.*, 2004] suggest that such iron may be susceptible to removal by the oxalate wash, or depending on the nature of the particle (for example lithogenic Fe bound within the organic matrix of a heterogeneous particle [*Lampitt et al.*, 1993]) may be "intracellular," i.e., not accessible by the oxalate wash. Like all wash (and digestion or filtration) methods, the oxalate technique is necessarily operationally defined, and further work will be needed to rigorously define what fractions of lithogenic and biogenic Fe are susceptible to removal by this method for various types of marine particles.

4.2. Comparison of Trends in Downward Particulate Fluxes With Other Studies

[41] During FeCycle, both trap arrays were in the SF_6-patch for over half of their 7-day deployment, and subsequently they remained within HNLC waters for days 6 and 7 of the deployment. Given the shallow deployment depth of the traps (80 and 120 m), and a calculated length scale of the source region for particles of 1.5–3.5 km for fast- and slow-sinking particles (assuming sinking speeds of 100 m d^{-1} and 35 m d^{-1}, respectively [*Siegel et al.*, 1990]), the traps would have predominantly sampled sinking particles that originated within the SF_6-labeled

patch. These export fluxes can therefore be compared with the suspended PFe data sets obtained during FeCycle, and related to previous studies in this region.

[42] The trap fluxes for POC, PON, POP and BSi during FeCycle were comparable to those from previous studies in the upper ocean (i.e., 100–150 m depth) in the New Zealand subantarctic region [*Nodder and Alexander*, 1998; *Nodder and Northcote*, 2001; S. D. Nodder, unpublished data, 2004]. There are no previous measurements of PFe export fluxes for the HNLC waters SE of New Zealand, and also few prior studies of downward PFe fluxes that may be compared with our results. PFe export during FeCycle ranged from 219 to 548 nmol m^2 d^{-1} at 80 m depth, much lower than PFe export studies in the Baltic Sea (annual range at 120 m depth was <10–140 μmol m^{-2} d^{-1} [*Pohl et al.*, 2004]) or in the Mediterranean (22–89 mmol m^{-2} d^{-1}, derived from a two-compartment box model [*Sarthou and Jeandel*, 2001]). These large differences are not surprising, considering the much smaller Fe supply to open-ocean subantarctic waters compared to these two coastal oceanic regimes [*de Baar and de Jong*, 2001]. Moreover, the elevated PFe export rates in other studies may also be due to the lack of application of procedural blanks (i.e., blank trap cylinders deployed concurrently with the open trap cylinders); for instance, *Pohl et al.* [2004] only measured DFe concentrations in trap brine, which in their study was on the order of 29 nM.

[43] The FeCycle export fluxes are also lower than upper ocean measurements in other Southern Ocean regions such as the Antarctic Peninsula (2.0 μmol m^{-2} d^{-1} [*Martin*, 1990]) and the polar SOIREE site S of Australia (4.7 μmol m^{-2} d^{-1} estimated for sinking non-biogenic (>99%) and biogenic (<1%) iron [*Bowie et al.*, 2001]). Interestingly, whereas *Bowie et al.* [2001] suggested that the nonbiogenic component, postulated to be in the form of insoluble iron hydroxides, was the dominant contributor to total PFe fluxes, during FeCycle we measured significant biogenic iron (>50%) in sinking particles (Table 4b). Thus the FeCycle biogenic PFe fluxes are higher than those estimated, using measured POC trap fluxes and an Fe:C ratio of 3 μmol Fe (mol C)$^{-1}$, by *Bowie et al.* [2001] during SOIREE both inside (i.e., waters subjected to multiple iron additions) and outside (i.e., HNLC polar waters) the iron-enriched mesoscale patch.

4.3. Comparison of Trends in the Mixed-Layer PFe Inventory and the Downward PFe Fluxes

[44] During FeCycle, we estimate that daily downward PFe fluxes were ~1% of the total PFe inventory in the surface mixed layer. This compares well with the estimates of 0.5–0.8% of the mixed-layer inventory for the downward PAl flux (data not shown). Moreover, the downward fluxes of POC, PON and POP were all <0.5% of surface layer inventory, with BSi being 1.9% (data not shown). We observed a threefold to fivefold increase in the particulate Fe:C (μmol:mol) ratio between the mixed layer and the traps at 80 m and 120 m depth (see Figure 5). The surface mixed layer is usually a region of particle production [*Boyd et al.*, 1999] with picophytoplankton being found in significant numbers in sinking particles from nearby HNLC subantarctic waters [*Waite et al.*, 2000]. Upon exiting the surface layer, biogenic particles are subjected to many transformations leading to a rapid vertical attenuation in particle fluxes, mainly due to microbial solubilization of particles [*Bidle and Azam*, 1999; *Bidle et al.*, 2002]. This attenuation of the particle flux is generally represented by a power law function [*Martin et al.*, 1987; *Bender et al.*, 1992]. It is also well established that different elements have different remineralization length scales [*Denman and Pena*, 2000], for example the length scale for C is longer than that for N owing to the preferential solubilization of N over C by heterotrophic bacteria [*Smith et al.*, 1992]. Likewise, a deeper remineralization profile is typical for particulate BSi compared to either C or N [*Denman and Pena*, 2000] owing to its mineral character, the need for heterotrophic bacteria to first remove organic C coatings (glycoproteins) from frustules prior to their dissolution, and the relative lack of biological demand for this element below the euphotic zone [*Tréguer et al.*, 1995, 2003].

[45] Thus the likely explanation for this trend in particulate Fe:C ratios in the upper 80 m during FeCycle is mechanistic differences in how C and Fe are remineralized. Sinking POC is rapidly converted to DOC owing to bacterial solubilization of particles [*Azam*, 1998], whereas PFe remineralized by microbial activity on particle surfaces and/or electrochemical gradients within particles [*Alldredge and Cohen*, 1987; *Wells et al.*, 1995] is probably immediately rescavenged onto particles in the upper ocean [*Clegg and Whitfield*, 1990] (also Figure 5, this study). The observed increase in particulate Fe:C ratios to 80 m depth (Figure 5) was more pronounced for particulate Fe:N ratios during FeCycle, which increased fourfold to fivefold from the mixed layer to the trap deployment depths (data not shown). This is consistent with the very rapid remineralization rates of N on sinking particles, as discussed above. In general, we suggest that the large increases in Fe:C and Fe:N particulate ratios we observed with depth are largely attributable to preferential losses of C and N relative to Fe during export.

[46] Similar processes occur for other particle-reactive elements such as Th, which has been selected as a model analog for the geochemical cycle of iron [*Parekh et al.*, 2004], and used to better follow and understand the dynamics of such elements subsequent to grazing [*Barbeau et al.*, 2001]. *Parekh et al.* [2004] put forward three conceptual models for the transformations between particulate and dissolved iron: one based on simple scavenging, one based on scavenging/desorption (by analogy to Th), and one including organic complexation. Our particulate Fe:C results from the upper FeCycle trap perhaps best fit the net scavenging scenario, with marked enrichment of Fe during export because there appears to be significant net rescavenging upon solubilization, in contrast to C and N. However, particle scavenging processes in the upper ocean typically yield to net remineralization as particle loads rapidly diminish with depth [*Whitfield and Turner*, 1987]. It is possible that the scavenging/desorption or complexation models of *Parekh et al.* [2004] would more accurately represent Fe biogeochemical transformations at depths

>80 m. Because of the different length-scales of remineralization of Fe and C, particulate Fe:C ratios would be expected to decrease as particles settle into the deep ocean. Removal of PFe (due to remineralization) would be expected to increase with depth as reflected by the shape of the DFe profiles at intermediate depths (i.e., >300 m) [*Laës et al.*, 2003].

4.4. Evidence for a Lithogenic to Biogenic Particle Transformation Pathway

[47] The magnitude of the downward PFe fluxes during a 7-day trap deployment at 80 m and 120 m depth (i.e., >30 m and 70 m below the mixed layer, respectively) are comparable to published dust deposition rates for this region (500 nmol Fe m^{-2} d^{-1}, derived from *Jickells and Spokes* [2001]); for a justification of the calculation of a daily dust flux from annual dust deposition rates, see *Boyd et al.* [2005]. Moreover, as the vertical diffusive and lateral advective supply terms for DFe were relatively small for FeCycle, it is possible to directly relate the magnitude of these two particulate terms [see *Boyd et al.*, 2005, Figure 3]. Correspondence between the magnitudes of these particulate Fe source and sink terms suggests that much of the dust entering the upper ocean might be exported directly to depth.

[48] However, a consideration of the lithogenic and biogenic components of these particulate fluxes separately does not support this scenario. The estimated daily atmospheric input of lithogenic Fe is greater than the measured daily lithogenic export to depth by twofold to fourfold (Table 4a). While there is no significant atmospheric source of biogenic particulates, the loss term due to export is 174–352 nmol Fe m^{-2} d^{-1}. In order to balance the supply and loss of both types of Fe, there must be a major pathway(s) converting lithogenic to biogenic Fe. Support for this notion also comes from the large decrease in the lithogenic:biogenic ratios of exported PFe compared with the suspended particles in the mixed layer.

[49] Residence times for lithogenic Fe in the surface mixed layers elsewhere have been calculated to be on the order of >10 days [*Croot et al.*, 2004; *Jickells*, 1999]. In FeCycle, the daily PFe export flux corresponds to 1% of the suspended PFe mixed-layer inventory. This yields an average residence time of particles in the mixed layer of ~100 days. The repartitioning of lithogenic Fe entering the surface ocean between size fractions is likely to be driven by a range of processes during this long residence time within the surface mixed layer (Figure 5). Candidate mechanisms include solubilization of mineral iron facilitated by bacterial siderophores [*Yoshida et al.*, 2002; *Brantley et al.*, 2004], grazing by mesozooplankton [*Hutchins and Bruland*, 1994], ingestion of Fe colloids or mineral particles by microzooplankton [*Barbeau et al.*, 1996; *Granger and Price*, 1999; *Barbeau and Moffett*, 2000], and incorporation of lithogenic material into Fe "hot spots" in organic particle aggregates [*Lam et al.*, 2004; *Twining et al.*, 2004]. Strong selective pressure in an Fe-limited environment has likely led to multiple routes by which lithogenic inputs may be accessed by the biota. That the biota can efficiently obtain PFe is not particularly surprising, given their demonstrated ability to develop mechanisms to obtain Fe from other forms such as strong iron/organic ligand complexes [*Hutchins et al.*, 1999; *Maldonado et al.*, 2005].

4.5. Biogeochemical Implications of a Lithogenic to Biogenic PFe Pathway

[50] This putative pathway would have widespread implications for the biogeochemical cycling of iron, in that PFe may be a significantly more available source than has been previously recognized. Our results suggest that passive dissolution of dust particles in the mixed layer is insufficient to explain the conversion of lithogenic to biogenic Fe, and that the biota must play an active role in this process. Using the global abiotic solubility of 1–10% for dust aerosols for the major desert regions [*Jickells and Spokes*, 2001], only 5–50 nmol Fe m^2 d^{-1} would become available for biological uptake in the mixed layer at this site, 1 to 2 orders of magnitude lower than the daily biogenic fluxes measured in the FeCycle sediment traps.

[51] How would such a lithogenic to biogenic transformation impact other ocean regions with higher lithogenic Fe inputs? These regions such as the subtropical and tropical Atlantic (with 2 orders of magnitude more dust supply [*Jickells and Spokes*, 2001]) have similarly low microbial stocks and hence low biogenic Fe [*Tortell et al.*, 1999], owing to the low biomass that can be supported in these macronutrient-limited oligotrophic waters [*Bory and Newton*, 2000; *Croot et al.*, 2004]. In regions such as these, it is likely that much of this lithogenic Fe will be directly exported as the ratio of lithogenic material to plankton biomass (i.e., the proportion of this lithogenic Fe that can be accessed during its upper ocean residence is dependent on microbial stocks) is much greater than in HNLC waters south of New Zealand. Indeed, a wide range of lithogenic fluxes have been reported in deep-moored sediment traps in the open ocean [*Francois et al.*, 2002].

References

Alldredge, A. L., and Y. Cohen (1987), Can microscale chemical patches persist in the sea? Microelectrode study of marine snow, fecal pellets, *Science*, *235*, 689–691.

Azam, F. (1998), Microbial control of oceanic carbon flux: The plot thickens, *Science*, *280*, 694–695.

Barbeau, K., and J. W. Moffett (2000), Laboratory and field studies of colloidal iron oxide dissolution as mediated by phagotrophy and photolysis, *Limnol. Oceanogr.*, *45*, 827–835.

Barbeau, K., J. W. Moffett, D. A. Caron, P. L. Croot, and D. L. Erdner (1996), Role of protozoan grazing in relieving iron limitation of phytoplankton, *Nature*, *380*, 61–64.

Barbeau, K., K. W. Bruland, and A. Butler (2001), Photochemical cycling of iron in the surface ocean mediated by microbial iron (III)-binding ligands, *Nature*, *413*, 409–413.

Bender, M., H. Ducklow, J. Kiddon, J. Marra, and J. Martin (1992), The carbon balance during the 1989 spring bloom in the North Atlantic Ocean, 47°N, 20°W, *Deep Sea Res., Part I*, *39*, 1707–1725.

Betzer, P. R., et al. (1988), Long-range transport of giant mineral aerosol particles, *Nature*, *336*, 568–572.

Bidle, K. D., and F. Azam (1999), Accelerated dissolution of diatom silica by marine bacterial assemblages, *Nature*, *397*, 508–512.

Bidle, K. D., M. Manganelli, and F. Azam (2002), Regulation of oceanic silicon and carbon preservation by temperature control on bacteria, *Science*, *298*, 1980–1984.

Bory, A. J. M., and P. P. Newton (2000), Transport of airborne lithogenic material down through the water column in two contrasting regions of the eastern subtropical North Atlantic Ocean, *Global Biogeochem. Cycles*, *14*(1), 297–315.

Bowie, A. R., M. T. Maldonado, R. D. Frew, P. L. Croot, E. P. Achterberg, R. F. C. Mantoura, P. J. Worsfold, C. S. Law, and P. W. Boyd (2001), The fate of added iron during a mesoscale fertilisation in the polar Southern Ocean, *Deep Sea Res., Part II*, *48*, 2703–2744.

Boyd, P. W., et al. (1999), Transformations of biogenic particulates from the pelagic to the deep ocean realm, *Deep Sea Res., Part II*, *46*, 2761–2792.

Boyd, P. W., et al. (2000), Mesoscale iron fertilisation elevates phytoplankton stocks in the polar Southern Ocean, *Nature*, *407*, 695–702.

Boyd, P. W., et al. (2004a), The decline and fate of an iron-induced subarctic phytoplankton bloom, *Nature*, *428*, 549–553.

Boyd, P. W., K. Richardson, V. Sherlock, M. Ellwood, and R. D. Frew (2004b), Episodic enhancement of phytoplankton stocks in New Zealand subantarctic waters: Contribution of atmospheric and oceanic iron supply, *Global Biogeochem. Cycles*, *18*, GB1029, doi:10.1029/2002GB002020.

Boyd, P. W., et al. (2005), FeCycle: Attempting an iron biogeochemical budget from a mesoscale SF_6 tracer experiment in unperturbed low iron waters, *Global Biogeochem. Cycles*, *19*, GB4S20, doi:10.1029/2005GB002494.

Bradford-Grieve, J. M., P. W. Boyd, F. H. Chang, S. Chiswell, M. Hadfield, J. A. Hall, M. R. James, S. D. Nodder, and E. A. Shushkina (1999), Pelagic ecosystem structure and functioning in the Subtropical Front region east of New Zealand in austral winter and spring 1993, *J. Plankton Res.*, *21*, 405–428.

Brantley, S. L., L. J. Liermann, R. L. Guynn, A. Anbar, G. A. Icopini, and J. Barling (2004), Fe isotopic fractionation during mineral dissolution with and without bacteria, *Geochim. Cosmochim. Acta*, *68*, 3189–3204.

Buesseler, K. O. (1991), Do upper-ocean sediment traps provide an accurate record of particle flux?, *Nature*, *353*, 420–423.

Buesseler, K. O., D. K. Steinberg, A. F. Michaels, R. J. Johnson, J. E. Andrews, J. R. Valdes, and J. F. Price (2000), A comparison of the quantity and composition of material caught in a neutrally buoyant versus surface tethered sediment trap, *Deep Sea Res., Part I*, *47*, 277–294.

Buesseler, K. O., J. E. Andrews, S. M. Pike, and M. A. Charette (2004), The effects of iron fertilization on carbon sequestration in the Southern Ocean, *Science*, *304*, 414–417.

Clegg, S. L., and M. Whitfield (1990), A generalized-model for the scavenging of trace-metals in the open ocean: 1. Particle cycling, *Deep Sea Res., Part I*, *37*, 809–832.

Coale, K. H., et al. (1996), A massive phytoplankton blooms induced by an ecosystem-scale iron fertilization experiment in the equatorial Pacific Ocean, *Nature*, *383*, 495–501.

Collier, R., and J. Edmond (1984), The trace element geochemistry of marine biogenic particulate matter, *Prog. Oceanogr.*, *13*, 113–199.

Croot, P. L., et al. (2004), Short residence time for iron in surface seawater impacted by atmospheric dry deposition from Saharan dust events, *Geophys. Res. Lett.*, *31*, L23S08, doi:10.1029/2004GL020153.

Cullen, J. T., and R. M. Sherrell (1999), Techniques for determination of trace metals in small samples of size-fractionated particulate matter: Phytoplankton metals off central California, *Mar. Chem.*, *67*, 233–247.

de Baar, H. J. W., and P. W. Boyd (1999), The role of iron in plankton ecology and carbon dioxide transfer of the global oceans, in *The Dynamic Ocean Carbon Cycle: A Midterm Synthesis of the Joint Global Ocean Flux Study*, edited by R. B. Hanson, H. W. Ducklow, and J. G. Field, pp. 61–140, Cambridge Univ. Press, New York.

de Baar, H. J. W., and J. T. M. de Jong (2001), Distributions, sources and sinks of iron in seawater, in *The Biogeochemistry of Iron in Seawater*, edited by D. Turner and K. A. Hunter, pp. 125–253, John Wiley, Hoboken, N. J.

de Baar, H. J. W., J. T. M. de Jong, R. F. Nolting, K. R. Timmermans, M. A. van Leeuwe, U. Bathmann, M. R. van der Loeff, and J. Sildam (1999), Low dissolved Fe and the absence of diatom blooms in remote Pacific waters of the Southern Ocean, *Mar. Chem.*, *66*, 1–34.

Denman, K. L., and M. A. Pena (2000), The dynamic ocean carbon cycle: A midterm synthesis of the Joint Global Ocean Flux Study, in *Beyond JGOFS*, edited by R. B. Hanson, H. W. Ducklow, and J. G. Field, pp. 469–490, Cambridge Univ. Press, New York.

Francois, R., S. Honjo, R. Krishfield, and S. Manganini (2002), Factors controlling the flux of organic carbon to the bathypelagic zone of the ocean, *Global Biogeochem. Cycles*, *16*(4), 1087, doi:10.1029/2001GB001722.

Fung, I. Y., et al. (2000), Iron supply and demand in the upper ocean, *Global Biogeochem. Cycles*, *14*(1), 281–296.

Gardner, W. D. (2000), Sediment trap sampling in surface waters, in *The Changing Ocean Carbon Cycle: A Midterm Synthesis of the Joint Global Ocean Flux Study*, edited by R. B. Hanson, H. W. Ducklow, and J. G. Field, pp. 240–281, Cambridge Univ. Press, New York.

Gnanadesikan, A., J. L. Sarmiento, and R. D. Slater (2003), Effects of patchy ocean fertilization on atmospheric carbon dioxide and biological production, *Global Biogeochem. Cycles*, *17*(2), 1050, doi:10.1029/2002GB001940.

Gordon, R. M., K. S. Johnson, and K. H. Coale (1998), The behavior of iron and other trace elements during the IronEx-I and PlumEx experiments in the equatorial Pacific, *Deep Sea Res., Part I*, *45*, 995–1041.

Granger, J., and N. M. Price (1999), The importance of siderophores in iron nutrition of heterotrophic marine bacteria, *Limnol. Oceanogr.*, *44*, 541–555.

Gust, G., et al. (1994), Mooring line motions and sediment trap hydromechanics-In-situ intercomparison of 3 common deployment designs, *Deep Sea Res., Part I*, *41*, 831–857.

Hesse, P. P., and G. H. McTainsh (1999), Last Glacial Maximum to early Holocene wind strength in the mid-latitudes of the Southern Hemisphere from aeolian dust in the Tasman Sea, *Quat. Res.*, *52*, 343–349.

Hudson, R. J. M., and F. M. M. Morel (1989), Distinguishing between extra- and intracellular iron in marine phytoplankton, *Limnol. Oceanogr.*, *34*, 1113–1120.

Hutchins, D. A., and K. W. Bruland (1994), Grazer-mediated regeneration and assimilation of Fe, Zn and Mn from planktonic prey, *Mar. Ecol. Prog. Ser.*, *110*, 259–269.

Hutchins, D. A., W. X. Wang, M. A. Schmidt, and N. S. Fisher (1999), Dual-labeling techniques for trace metal biogeochemical investigations in aquatic plankton communities, *Aquat. Microbiol. Ecol.*, *19*, 129–138.

Jickells, T. D. (1999), The inputs of dust derived elements to the Sargasso Sea: A synthesis, *Mar. Chem.*, *68*, 5–14.

Jickells, T. D., and L. J. Spokes (2001), Atmospheric iron inputs to the oceans, in *The Biogeochemistry of Iron in Seawater*, edited by D. Turner, and K. A. Hunter, pp. 85–122, John Wiley, Hoboken, N. J.

Johnson, K. S., et al. (1997), What controls dissolved iron concentrations in the world ocean?, *Mar. Chem.*, *57*, 137–161.

Karl, D. M., C. D. Winn, D. V. W. Hebel, and R. Letelier (1990), Sediment trap protocol, in *Hawaii Ocean Time-Series Program Field and Laboratory Protocols*, pp. 66–69, U.S. JGOFS Program Office, Natl. Sci. Found., Washington, D. C.

Knauer, G. A., D. M. Karl, J. H. Martin, and C. N. Hunter (1984), In situ effects of selected preservatives on total carbon, nitrogen and metals collected in sediment traps, *J. Mar. Res.*, *42*, 445–462.

Kumar, N., R. F. Anderson, R. A. Mortlock, P. N. Froelich, P. Kubik, B. Dittrich-Hannen, and M. Suter (1995), Increased biological productivity and export production in the glacial Southern Ocean, *Nature*, *378*, 675–680.

Kuss, J., and K. Kremling (1999), Spatial variability of particle associated trace elements in near-surface waters of the North Atlantic (30°N/60°W to 60°N/2°W), derived by large-volume sampling, *Mar. Chem.*, *68*, 71–86.

Laës, A., S. Blain, P. Laan, E. P. Achterberg, G. Sarthou, and H. J. W. de Baar (2003), Deep dissolved iron profiles in the eastern North Atlantic in relation to water masses, *Geophys. Res. Lett.*, *30*(17), 1902, doi:10.1029/2003GL017902.

Lam, P. J., J. K. Bishop, G. A. Waychunas, and M. A. Marcus (2004), Iron hotspots in marine aggregates of the subarctic Pacific, paper presented at 2004 Ocean Research Conference, Am. Soc. of Limnol. and Oceanogr., Waco, Tex.

Lampitt, R. S., K. F. Wishner, C. M. Turley, and M. V. Angel (1993), Marine snow studies in the Northeast Atlantic Ocean: Distribution, composition and role as a food source for migrating plankton, *Mar. Biol.*, *116*, 689–702.

Lebo, M. E., and J. H. Sharp (1992), Modeling phosphorus cycling in a well-mixed coastal-plain estuary, *Estuarine Coastal Shelf Sci.*, *35*, 235–252.

Mackie, D. S., P. W. Boyd, K. A. Hunter, and G. H. McTainsh (2005), Simulating the cloud processing of iron in Australian dust: pH and dust concentration, *Geophys. Res. Lett.*, *32*, L06809, doi:10.1029/2004GL022122.

Maldonado, M. T., R. F. Strzepek, S. Sander, and P. W. Boyd (2005), Acquisition of iron bound to strong organic complexes, with different Fe binding groups and photochemical reactivities, by plankton communities in Fe-limited subantarctic waters, *Global Biogeochem. Cycles*, *19*, GB4S23, doi:10.1029/2005GB002481.

Martin, J. H. (1990), Glacial-interglacial CO_2 change: The iron hypothesis, *Paleoceanography*, *5*, 1–13.

Martin, J. H., G. A. Knauer, D. M. Karl, and W. W. Broenkow (1987), VERTEX - carbon cycling in the northeast Pacific, *Deep Sea Res., Part I*, *34*, 267–285.

Martin, J. H., R. M. Gordon, S. Fitzwater, and W. W. Broenkow (1989), VERTEX: Phytoplankton/iron studies in the Gulf of Alaska, *Deep Sea Res., Part I*, *36*, 649–680.

Martin, J. H., S. Fitzwater, and R. M. Gordon (1990), Iron deficiency limits phytoplankton growth in Antarctic waters, *Global Biogeochem. Cycles*, *4*(1), 5–12.

Martin, J. H., et al. (1994), Testing the iron hypothesis in ecosystems of the equatorial Pacific Ocean, *Nature*, *371*, 123–129.

McGowan, H. A., G. H. McTainsh, and P. Zawar-Reza (2000), Identifying regional dust transport pathways: Application of kinematic trajectory modelling to a trans-Tasman case, *Earth Surf. Processes Landforms*, *25*, 633–647.

McGowan, H. A., B. Kamber, G. H. McTainsh, and S. K. Marx (2005), High resolution provenancing of long travelled dust deposited on the Southern Alps, New Zealand, *Geomorphology*, *69*(1–4), 208–221.

McKay, R. M. L., W. Wilhelm, J. Hall, D. A. Hutchins, M. M. D. Al-Rshaidat, C. E. Mioni, S. Pickmere, D. Porta, and P. W. Boyd (2005), Impact of phytoplankton on the biogeochemical cycling of iron in subantarctic waters southeast of New Zealand during FeCycle, *Global Biogeochem. Cycles*, *19*, GB4S24, doi:10.1029/2005GB002482.

Mills, M. M., C. Ridame, M. Davey, J. La Roche, and R. J. Geider (2004), Iron and phosphorus co-limit nitrogen fixation in the eastern tropical North Atlantic, *Nature*, *429*, 292–294.

Minagawa, M., D. A. Winter, and I. R. Kaplan (1984), Comparison of Kjeldahl and combustion methods for measurement of nitrogen isotope ratios in organic matter, *Anal. Chem.*, *56*, 1859–1861.

Nelson, D. M., W. O. J. Smith, R. D. Muench, L. I. Gordon, C. W. Sullivan, and D. M. Husby (1989), Particulate matter and nutrient distributions in the ice-edge zone of the Weddell Sea: Relationship to hydrography during late summer, *Deep Sea Res., Part I*, *36*, 191–209.

Nishioka, J., S. Takeda, C. S. Wong, and W. K. Johnson (2001), Size-fractionated iron concentrations in the northeast Pacific Ocean: Distribution of soluble and small colloidal iron, *Mar. Chem.*, *74*, 157–179.

Nodder, S. D., and B. L. Alexander (1998), Sources of variability in geographical and seasonal differences in particulate fluxes from short-term sediment trap deployments, east of New Zealand, *Deep Sea Res., Part I*, *45*, 1739–1764.

Nodder, S. D., and L. C. Northcote (2001), Episodic particulate fluxes at southern temperate mid-latitudes (42–45°S) in the Subtropical Front region, east of New Zealand, *Deep Sea Res., Part I*, *48*, 833–864.

Parekh, P., M. J. Follows, and E. Boyle (2004), Modeling the global iron cycle, *Global Biogeochem. Cycles*, *18*, GB1002, doi:10.1029/2003GB002061.

Pohl, C., A. Loffler, and U. Hennings (2004), A sediment trap flux study for trace metals under seasonal aspects in the stratified Baltic Sea (Gotland Basin; 57°19.20′N; 20°03.00′E), *Mar. Chem.*, *84*, 143–160.

Price, N. M., and F. M. M. Morel (1998), Biological cycling of iron in the ocean, in *Metal Ions in Biological Systems*, *Iron Transport Microorganisms*, vol. 35, edited by A. Sigel and H. Sigel, pp. 1–36, CRC Press, Boca Raton, Fla.

Prospero, J. M., M. Uematsu, and D. L. Savoie (1989), Mineral aerosol transport to the Pacific Ocean, in *Chemical Oceanography*, vol. 10, edited by J. P. Riley, R. Chester, and R. A. Duce, pp. 187–218, Elsevier, New York.

Quétel, C. R., E. Remoudaki, J. E. Davies, J. C. Miquel, S. W. Fowler, C. E. Lambert, G. Bergametti, and P. Buatmenard (1993), Impact of atmospheric deposition on particulate iron flux and distribution in northwestern Mediterranean waters, *Deep Sea Res., Part I*, *40*, 989–1002.

Ragueneau, O., et al. (2000), A review of the Si cycle in the modern ocean: Recent progress and missing gaps in the application of biogenic opal as a paleoproductivity proxy, *Global Planet. Change*, *26*, 317–365.

Sarthou, G., and C. Jeandel (2001), Seasonal variations of iron concentrations in the Ligurian Sea and iron budget in the western Mediterranean Sea, *Mar. Chem.*, *74*, 115–129.

Sherrell, R. M., and E. A. Boyle (1992), The trace metal composition of suspended particles in the oceanic water column near Bermuda, *Earth Planet. Sci. Lett.*, *111*, 155–174.

Siegel, D. A., T. C. Granata, A. F. Michaels, and T. D. Dickey (1990), Mesoscale eddy diffusion, particle sinking, and the interpretation of sediment trap data, *J. Geophys. Res.*, *95*, 5305–5311.

Smith, D. C., M. Simon, A. L. Alldredge, and F. Azam (1992), Intense hydrolytic enzyme activity on marine aggregates and implications for rapid particle dissolution, *Nature*, *359*, 139–142.

Spokes, L. J., and T. D. Jickells (1996), Factors controlling the solubility of aerosol trace metals in the atmosphere and on mixing into seawater, *Aquat. Geochem.*, *1*, 355–374.

Strzepek, R. F., M. T. Maldonado, J. L. Higgins, J. Hall, K. Safi, S. W. Wilhelm, and P. W. Boyd (2005), Spinning the "Ferrous Wheel": The importance of the microbial community in an iron budget during the FeCycle experiment, *Global Biogeochem. Cycles*, *19*, GB4S26, doi:10.1029/2005GB002490.

Tortell, P. D., M. T. Maldonado, J. Granger, and N. M. Price (1999), Marine bacteria and biogeochemical cycling of iron in the oceans, *FEMS Microbiol. Ecol.*, *29*, 1–11.

Tovar-Sanchez, A., S. A. Sañudo-Wilhelmy, M. Garcia-Vargas, R. S. Weaver, L. C. Popels, and D. A. Hutchins (2003), A trace metal clean reagent to remove surface-bound iron from marine phytoplankton, *Mar. Chem.*, *82*, 91–99.

Tréguer, P., D. M. Nelson, A. J. van Bennekom, D. J. DeMaster, A. Leynaert, and B. Quéginer (1995), The silica balance in the world ocean: A reestimate, *Science*, *268*, 375–379.

Tréguer, P., L. Legendre, R. T. Rivkin, O. Ragueneau, and N. Dittert (2003), Water column biogeochemistry below the euphotic zone, in *Ocean Biogeochemistry–The Role of the Ocean Carbon Cycle in Global Change*, edited by M. J. R. Fasham, pp. 145–156, Springer, New York.

Twining, B. S., S. B. Baines, and N. S. Fisher (2004), Element stoichiometries of individual plankton cells collected during the Southern Ocean Iron Experiment (SOFeX), *Limnol. Oceanogr.*, *49*, 2115–2128.

Waite, A. M., K. A. Safi, J. A. Hall, and S. D. Nodder (2000), Mass sedimentation of picoplankton embedded in organic aggregates, *Limnol. Oceanogr.*, *45*, 87–97.

Watson, A. J., D. C. E. Bakker, P. W. Boyd, A. J. Ridgwell, and C. S. Law (2000), Effect of iron supply on Southern Ocean CO_2 uptake and implications for glacial atmospheric CO_2, *Nature*, *407*, 730–734.

Wedepohl, K. H. (1995), The composition of the continental crust, *Geochim. Cosmochim. Acta*, *59*, 1217–1232.

Weinstein, S. E., and S. B. Moran (2004), Distribution of size-fractionated particulate trace metals collected by bottles and in-situ pumps in the Gulf of Maine–Scotian Shelf and Labrador Sea, *Mar. Chem.*, *87*, 121–135.

Wells, M. L., N. M. Price, and K. W. Bruland (1995), Iron chemistry in seawater and its relationship to phytoplankton: A workshop report, *Mar. Chem.*, *48*, 157–182.

Whitfield, M., and D. R. Turner (1987), The role of particles in regulating the composition of seawater, in *Aquatic Surface Chemistry*, edited by W. Stumm, pp. 457–493, John Wiley, Hoboken, N. J.

Wu, J. F., and E. Boyle (2002), Iron in the Sargasso Sea: Implications for the processes controlling dissolved Fe distribution in the ocean, *Global Biogeochem. Cycles*, *16*(4), 1086, doi:10.1029/2001GB001453.

Yoshida, T., K. Hayashi, and H. Ohmoto (2002), Dissolution of iron hydroxides by marine bacterial siderophore, *Chem. Geol.*, *184*, 1–9.

P. W. Boyd, National Institute of Water and Atmospheric Research, Centre for Chemical and Physical Oceanography, Department of Chemistry, University of Otago, Dunedin 9001, New Zealand. (pboyd@alkali.otago.ac.nz)

R. D. Frew, Department of Chemistry, University of Otago, P. O. Box 56, Dunedin 9001, New Zealand. (rfrew@alkali.otago.ac.nz)

C. E. Hare, D. A. Hutchins, and K. Leblanc, Graduate College of Marine Studies, University of Delaware, Lewes, DE 19958, USA. (chare@cms.udel.edu; dahutch@cms.udel.edu; leblanc@com-univ-mrs.fr)

S. Nodder, National Institute of Water and Atmospheric Research, Greta Point, Wellington, New Zealand. (s.nodder@niwa.cri.nz)

S. Sanudo-Wilhelmy, Marine Sciences Research Center, Stony Brook University, Stony Brook, NY 11794-5000, USA. (ssanudo@notes.cc.sunysb.edu)

A. Tovar-Sanchez, Instituto Mediterraneo de Estudios Avanzados (IMEDEA), Esporles E-07170, Mallorca, Spain. (antonio.tovar@uib.es)